THE IMPACT OF CLIMATE CHANGE ON SONAR PERFORMANCE: A CASE STUDY IN THE HIGH NORTH

V.O. Oppeneer TNO, The Hague, The Netherlands
N. Risser TNO, The Hague, The Netherlands
R. van Vossen TNO, The Hague, The Netherlands
K. Pelekanakis TNO, The Hague, The Netherlands
G. Giorli CMRE, La Spezia, Italy
A. Russo CMRE, La Spezia, Italy

1 INTRODUCTION

It is currently well known that climate change is affecting the Earth [1]. About 90% of the added heat energy resulting from anthropogenic perturbations (e.g. greenhouse gases) is absorbed by the oceans [2] [3]. Consequently, the oceans' temperatures are increasing globally. In polar regions this is accompanied with the melting of ice, which impacts the salinity gradients. These trends have local differences and depend on the area of interest (cf. chapter 2). This phenomenon affects the propagation of sound, and consequently sonar performance [4]. Oceanographic conditions are not the only factor affecting sonar performance. Wind, rain, biology, and anthropogenic sources such as shipping also contribute and must be taken into. In this work, climate change is related to sonar performance. A top-down approach is developed in a block diagram which relates climate change to sonar. Finally, this approach is illustrated using a passive sonar scenario case study in the high north.

2 CLIMATE CHANGE AND ITS RELATION TO SONAR PERFORMANCE

Ocean temperature affects the acoustic sound propagation as well as other factors also contributing to the performance of a sonar system. Figure 1 presents a comprehensive approach relating climate change to sonar performance. This happens in several stages, climate change and human activities affect the Acoustic Environment, which describes all the important factors necessary to determine the Ocean Acoustics. The Ocean Acoustics describes the propagation, scattering and noise. Finally, the Ocean Acoustics affects the Sonar Performance, both on the signal and the noise side.

The block diagram from Figure 1 can be used to analyse the impact of climate change in the area of interest, and gives insight in what literature or knowledge is necessary.
Many institutes do climate modelling to compute the oceanography (temperature, salinity, pH) for a future date, [1], [5], [6]. Similar work is done for the wind and rain [7], [8], [9], although results do not always agree [10], [11].
However, future biology and shipping activities are hard to predict. The presence of a species depends on the oceanography, the overall ecosystem, and the presence of human activity as fishing.

Most of the biology studies are conducted on few species, and to the best of our knowledge, there is no overarching work done on the change of animal and plankton distributions for future scenarios.
Concerning marine traffic activity, we can separate it within shipping, leisure, and fishing.
On one hand, the presence of fishing boats (and therefore the noise produced by them) depends on the presence of preys to capture, for which no real prediction is available. On the other hand, new commercial shipping routes are expected to open in the Arctic [12].
There is currently a lot of work being done on predicting the sea ice coverage in the Arctic. Predictions support a decrease in the ice sea coverage, more important in summer than in winter, [13], [14]. Eventually, the Arctic is predicted to be ice-free in summer time, even if all prediction don't always agree of when this will happens or for how many months [15], [16], [17].

When enough information is gathered on the Acoustic Environment, modelling for scattering, propagation, and ambient noise can be applied to compute the relevant inputs for a sonar performance calculation.

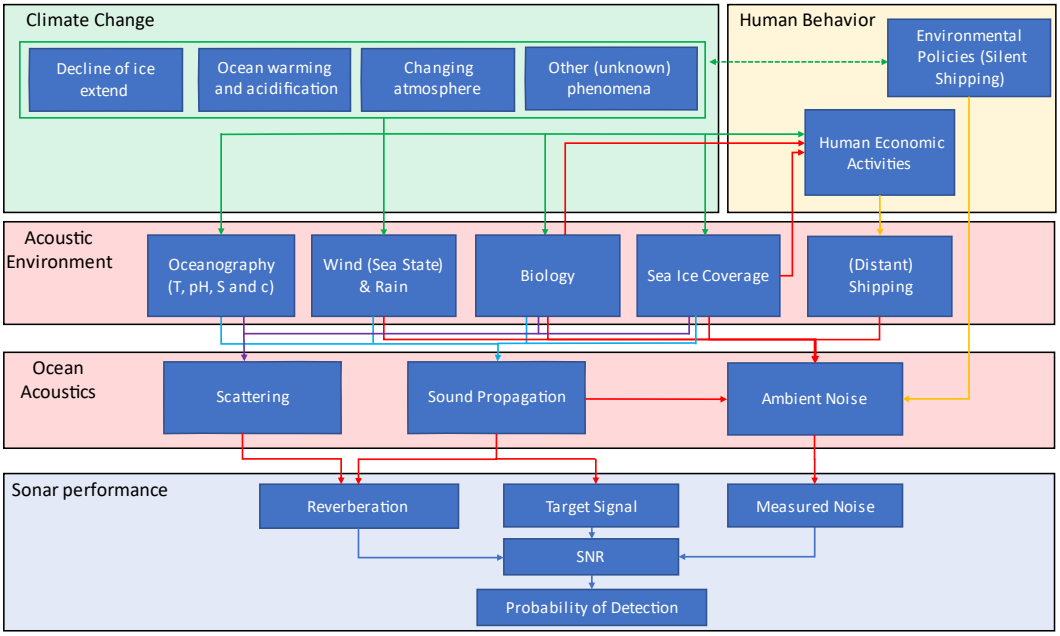

Figure 1. A block diagram, relating climate change to sonar performance. Arrows indicate how different blocks interlink with each other but not the strength of the link.

3 A PASSIVE SONAR CASE STUDY IN THE NORTH ATLANTIC

3.1 Scenario description

The scenario that will be considered here is a passive sonar scenario. This means solving the passive sonar equation, which can be written as [18], [19], [4]:

$$SNR = RNL - PL - NL + AG, \tag{1}$$

where SNR denotes the signal-to-noise ratio in a given frequency band. RNL is the radiated noise level, the sound radiated by the object of interest. PL is the propagation loss. NL is the ambient noise level, which is a combination of sea state noise (wind noise), rain noise, and shipping noise and AG is the array gain. The SNR can be converted to a probability of detection using equation 7.34 of [19] as:

$$p_d = p_{fa}^{\frac{1}{1+R}}, \tag{2}$$

where p_d is the probability of detection, p_{fa} is the probability of false alarm, and R is the linear SNR computed as: $R = 10^{\frac{SNR}{10}}$. p_{fa} which is assumed to be 10^{-5}. Furthermore, the detection range in this work is assumed to be the largest distance for which $p_d = 0.5$.

In the scenario, a latitude of 76 degrees and a longitude of 10 degrees are chosen, where the water depth is 2200 m, as reported in [20]. The sediment is assumed for this case study to be medium sand (with properties described in [19]).

A single hydrophone receiver at 30 meters depth is placed at these coordinates. The hydrophone is assumed to have a 1 s integration time, resulting in a processing bandwidth of 1 Hz.

Furthermore, a submerged target is located at 40 m depth. It has two tonals, based on [21]. The first tonal is at 63.096 Hz, bandwidth is 0.1 Hz, and the integrated radiated noise level over this bandwidth is 130 dB re μPa^2m^2. The second tonal is at 6309.6 Hz, same bandwidth, and the same integrated radiated noise level. It is assumed that these tonals have top-hat spectra: constant value within the bandwidth, zero outside of it. The integration bandwidth of the receiver is wide enough to capture all the energy of the tonals.

The oceanography is described in 3.2. Wind and rain distributions is described in 3.3. Biology is not considered in this study. Distant shipping is described in 3.4.

3.2 Oceanography

The area is the same as location 1 in [20], where the temperature and salinity were extracted from the outputs generated by the HadGEM3-GC31-HH model [22], part of the High Resolution Model Intercomparison Project [23]. The HadGEM3-GC31-HH model is based on the RCP8.5 scenario (worst case climatic scenario) [24], which assumes that the average temperature is going to increase 4.4C by 2100. Figure 2 showsthe average sound-speed-profiles for three years: 1995, 2020, and 2045. Multiple years are represented (dotted lines) with their average (filled coloured lines). The SSPs (Sound Speed Profiles) are similar within each decade and their average is a good representation, as it could be one of them. An acoustic duct is present within the first 45 meters, after which the sound speed decreases until reaching its minimum around 700m depth. If the shape is similar, the values themselves and the gradient change. There is a general increase of sound speed over time, especially between the surface and 700 m (minimum) with a difference of about 15 m/s in 1995 and about 30 m/s in 2045 (Figure 2).

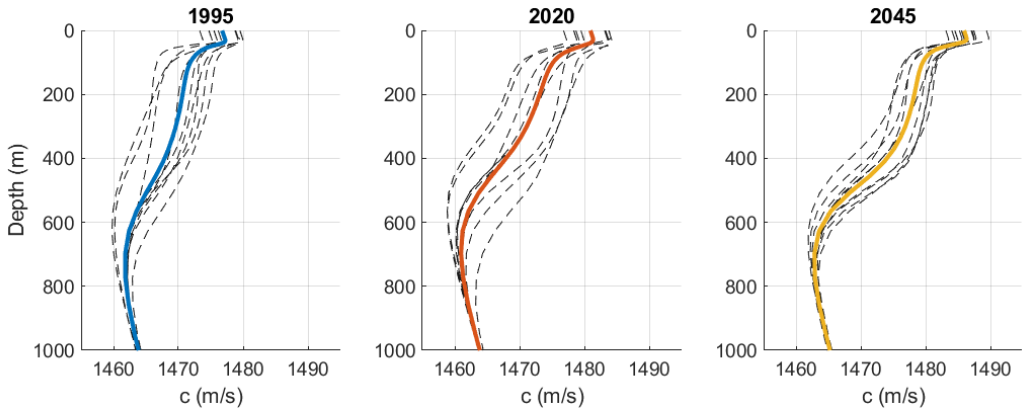

Figure 2. Sound speed profile (SSP) at the location of study. The year mentioned is the central year, the dashed lines are SSPs from 4 years before and after the central one and the solid colored lines are averages. After the first 1000 m, the curves collapse to the same increasing sound speed curve.

3.3 Wind and rain

Wind and rain distributions were generated using the atmospheric component of the same climate model [22] considered for oceanography and are shown in figure 3. Although it is not true, in this work it is assumed that windspeed and rain are independent of each other. From [25] it is known that most storms happen within 30 to 90 minutes, for the intents and purposes of this work it is assumed that all the precipitation of the day happens in a one hour interval (meaning that 23/24 hours of the day there is no rain). Between 1990s and the 2020s, the wind distribution has shifted toward higher wind speed with a slightly less high centre. However, between 2020s and 2040s, the difference is thinner than expected. Concerning the precipitation, in 2020s there is a higher density of low precipitation than in 1990s and 2040s. However, the slopes have quite similar shapes. The contribution from rain and wind to the modulation of SNR is therefore expected to be quite low.

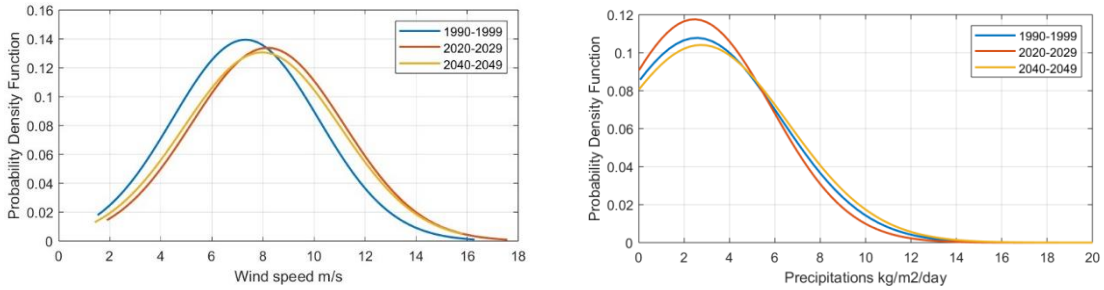

Figure 3. Probability density function of wind and rain at the location of study. The lines represent the average wind and rain for the month of September in the given decades.

3.4 Distant shipping noise

For the modelling of distant shipping noise, an implementation of the CANARY model [26] is used. Here all ships are assumed to be merchant container ships, where [27] present a formula (equation 10) for the mean spectrum per decidecade band. These can be converted to the 1 Hz bandwidth (for our receiver bandwidth) of the two frequencies for our case study. Furthermore, these ships are assumed to be a point source at 6 m depth.

Over time the number of ships in the area will increase [28]. It is expected that ships will get quieter, but currently there is no work that quantifies this reduction and is therefore currently ignored.
For the period of 2013-2019 it is reported that shipping noise increases linearly in the Barents Sea [28]. Our implementation of the CANARY model requires shipping densities as input. The linear relationship of the noise levels was extrapolated to 1995, 2020, and 2045. From these extrapolated noise levels, an estimation was done to determine what the corresponding average shipping density would have been. For these years the average shipping density per square kilometre are: 0 ships per km^2 in 1995; $1.3*10^{-5}$ ships per km^2 in 2020; and $1.8*10^{-2}$ ships per km^2 in 2045. Although this increase in ships may seem unrealistic, one should not forget that the region of interest will most likely be close to a future major shipping lane, when the Arctic becomes free of ice.

4 RESULTS AND DISCUSSION

4.1 Propagation loss

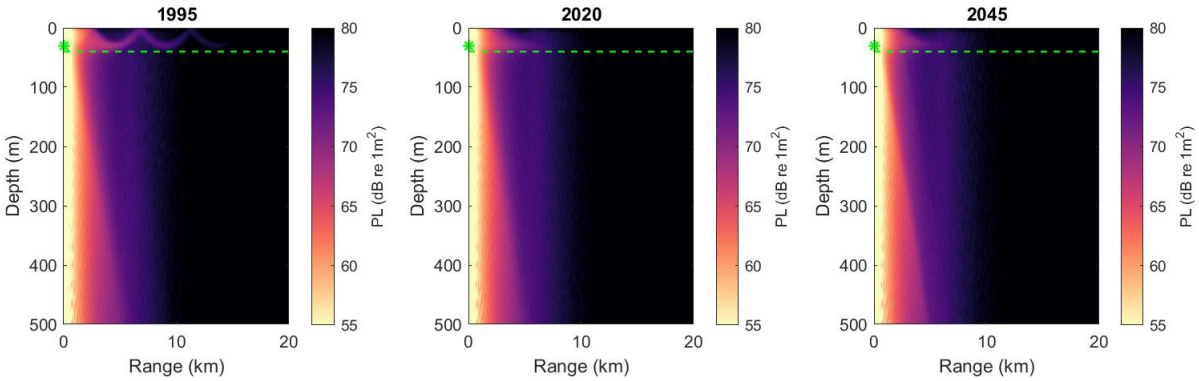

Figure 4. Propagation loss for the month of September in the three years. The frequency is 6309 Hz. The surface is assumed to be flat. The receiver is the green star, and the target is at the green dashed line.

Propagation loss was computed using two models, RAM for the lower frequency [29], and for the high frequency an incoherent ray model called INDRA [30] using a range independent SSP. The high frequency results for the three considered years are plotted in Figure 4, with a similar result for the low frequency. Although the receiver is inside the (weak) surface duct, it seems that the propagation

changes only a little bit at the target depth throughout the years. The surface duct seems to become weaker, and more acoustical energy leaks towards deeper depths.

4.2 Noise levels

The noise is a combination of shipping noise, wind noise (sea state noise), and rain noise. Biological sources of noise are not considered here. The noise distributions for our case study are presented in Figure 5.
At the low frequency, the 1990s case includes wind and rain noise. In 2020s, there is some shipping activity, raising the lowest noise levels to about 67 dB. In 2045, the wind and rain have don't have influence anymore and the shipping noise constitute all of the noise. This leads to a very thin peak, around 98 dB.
For the high frequency, the noise levels lie very close together. The shipping noise does not have an influence anymore, and the differences in noise are only due to the changes in wind and rain distributions. These changes in distributions are much smaller than the change in the number of ships, which mostly affect the 63.096 Hz scenario.

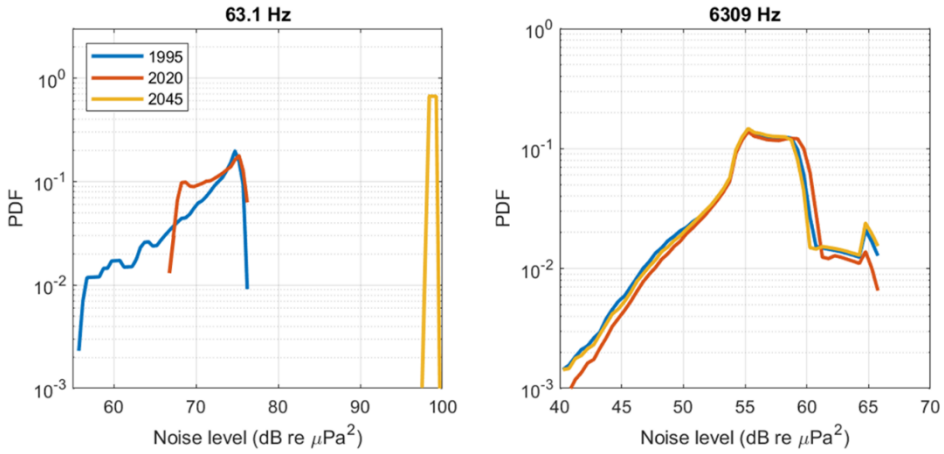

Figure 5. Noise level distribution as function of the year for two different frequencies (63.1Hz and 6309Hz). These are a combination of shipping noise, wind noise, and rain noise; received at the receiver location.

4.3 Detection range distributions

Combining the propagation, the noise levels, and the source level of the submerged vessel, one can compute the SNR and convert that to the probability of detection. The detection range is defined as the range for which the probability of detection equals 0.5. The cumulative probability density function (CDF) of detection range is shown in Figure 6. Where a value of 0 at a range means there are no detection ranges smaller than this range, and a value of 1 means there are no detection ranges above this range. From the receiver's perspective ideally, the CDF stays 0 as long as possible and only at long ranges it increases and goes to 1.
For the 63.096 Hz case, there is a big difference in the detection ranges over the year. This is because over the years the increased shipping changes the noise levels so significantly, that the tonal cannot be heard at all in 2040s, no matter the distance. In 2020s the detection ranges are worse than in 1995 with a CDF always higher for each range.

For the high frequencies, the CDFs lie almost on top of each, with slight differences due to changing wind and rain distributions, in combination with a slightly different SSP.
However, the changes in the SSP are relatively small, the overall shape is similar, only the absolute values and the values of the gradients change. In [31] it is show that in certain areas ducts can appear or disappear due to changes in the oceanography. It is expected that if the SSP changes in shape, the detection ranges for the high frequencies could also change.

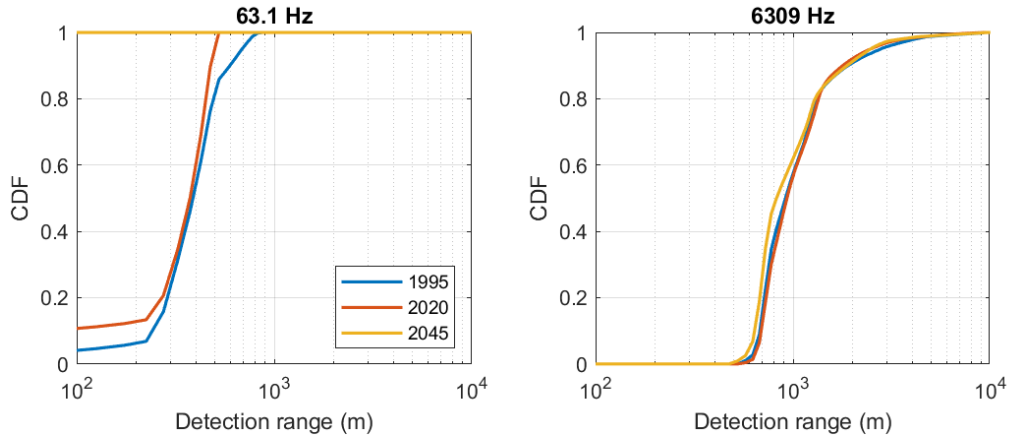

Figure 6. Detection ranges as CDFs. A CDF(r)=0 means no detection ranges are smaller than this r. A CDF(r)=1 means that there are no detection ranges larger than this r. Left: 63.096 Hz. Right: 6309.6 Hz.

5 CONCLUSIONS

In this work a block diagram is presented which links climate change to sonar performance. Climate change affects the acoustic environment, which impacts the ocean acoustics, and finally the sonar performance is influenced. Different amounts of literature and knowledge is available on how climate change affects the acoustic environment.

The method of decomposing the problem into blocks (Figure 1) and finding corresponding data for the past, present, and future was used to do a passive sonar case study in the north Atlantic, towards the arctic. A submerged vessel was held at constant depth of 40 m, and a single hydrophone receiver was placed at a constant depth of 30 m; both of which were inside a weak surface duct. The changing environment caused very little change in acoustic propagation. The noise statistics show that the biggest changes are at the low frequency, due to the large, expected increase in ships in this area. Similarly, the detection ranges were analysed. At the high frequencies there were barely any differences in the detection ranges. For the low frequency the detection ranges are becoming shorter through the years, in this case mostly driven by the increase in shipping noise.

This case study shows that it is important to look at all the components of the sonar equation, not just propagation, to determine future performances. Furthermore, this analysis of looking at all parts that contribute to the sonar performance is an important tool to explore what locations around the globe are affected by climate change. It would therefore be of interest to do similar work for more regions around the globe, for more frequencies, at different times of year, and for other target and receiver depths.

6 AKNOWLEDGEMENTS

The authors acknowledge the support and funding from the Netherlands Ministry of Defence, from the NATO Office of the Chief Scientist and of the Richard Lounsbery Foundation.

7 REFERENCES

[1] K. Calvin, D. Dasgupta, G. Krinner and e. al, IPCC, 2023: Climate Change 2023: Synthesis Report. Contribution of Working Groups I, II and III to the Sixth Assessment Report of the IPCC, Geneva, Switzerland, 2023.

[2] S. Levitus, J. I. Antonov, T. P. Boyer, O. K. Baranova, H. E. Garcia, R. A. Locarnini, A. V. Mishonov, J. R. Reagan, D. Seidov, E. S. Yarosh and M. M. Zweng, "World ocean heat content and thermosteric sea level change (0–2000 m), 1955–2010," *Geophysical Research Letters,* vol. 39, May 2012.

[3] K. von Schuckmann, A. Minière, F. Gues, F. J. Cuesta-Valero and e. al, "Heat stored in the Earth system 1960–2020: where does the energy go?," *Earth System Science Data,* vol. 15, p. 1675–1709, April 2023.

[4] F. Jensen, W. Kuperman, M. Porter and H. Schmidt, Computational Ocean Acoustics, Springer, 2011.

[5] J. Cos, F. Doblas-Reyes, M. Jury, R. Marcos, P.-A. Bretonnière and M. Samsó, "The Mediterranean climate change hotspot in the CMIP5 and CMIP6 projections," *Earth System Dynamics,* vol. 13, p. 321–340, February 2022.

[6] T. P. Sasse, B. I. McNeil, R. J. Matear and A. Lenton, "Quantifying the influence of CO2 seasonality on future aragonite undersaturation onset," *Biogeosciences,* vol. 12, p. 6017–6031, October 2015.

[7] M. Reale, W. Cabos Narvaez, L. Cavicchia and e. al, "Future projections of Mediterranean cyclone characteristics using the Med-CORDEX ensemble of coupled regional climate system models," *Climate Dynamics,* vol. 58, p. 2501–2524, November 2021.

[8] J. Debernard, Ø. Sætra and L. P. Røed, "Future wind, wave and storm surge climate in the northern North Atlantic," *Climate Research,* vol. 23, p. 39–49, 2002.

[9] G. Zappa, M. K. Hawcroft, L. Shaffrey, E. Black and D. J. Brayshaw, "Extratropical cyclones and the projected decline of winter Mediterranean precipitation in the CMIP5 models," *Climate Dynamics,* vol. 45, p. 1727–1738, December 2014.

[10] M. Andres-Martin, C. Azorin-Molina, C. Shen, J. C. Fernández-Alvarez, L. Gimeno, S. M. Vicente-Serrano and J. Zha, "Uncertainty in surface wind speed projections over the Iberian Peninsula: CMIP6 GCMs versus a WRF-RCM," *Annals of the New York Academy of Sciences,* vol. 1529, p. 101–108, September 2023.

[11] S. B. Power, F. Delage, R. Colman and A. Moise, "Consensus on Twenty-First-Century Rainfall Projections in Climate Models More Widespread than Previously Thought," *Journal of Climate,* vol. 25, p. 3792–3809, June 2012.

[12] R. Rowe, "The Northwest Passage - What is its status under the international law of the sea," UK Pandi, 27 Feb 2019. [Online]. Available: from https://www.ukpandi.com/news-and-resources/articles/2019/legal-article-the-northwest-passage---what-is-its-status-under-the-international-law-of-the-sea/. [Accessed 3 April 2024].

[13] D. Notz and J. Stroeve, "Observed Arctic sea-ice loss directly follows anthropogenic CO 2 emission," *Science,* vol. 354, p. 747–750, November 2016.

[14] J. C. Stroeve, V. Kattsov, A. Barrett, M. Serreze, T. Pavlova, M. Holland and W. N. Meier, "Trends in Arctic sea ice extent from CMIP5, CMIP3 and observations," *Geophysical Research Letters,* vol. 39, August 2012.

[15] J. E. Overland and M. Wang, "When will the summer Arctic be nearly sea ice free?," *Geophysical Research Letters,* vol. 40, p. 2097–2101, May 2013.

[16] F. Massonnet, T. Fichefet, H. Goosse, C. M. Bitz, G. Philippon-Berthier, M. M. Holland and P.-Y. Barriat, "Constraining projections of summer Arctic sea ice," *The Cryosphere,* vol. 6, p. 1383–1394, November 2012.

[17] Y. Aksenov, E. E. Popova, A. Yool, A. J. G. Nurser, T. D. Williams, L. Bertino and J. Bergh, "On the future navigability of Arctic sea routes: High-resolution projections of the Arctic Ocean and sea ice," *Marine Policy,* vol. 75, p. 300–317, January 2017.

[18] D. Abraham, Underwater Acoustic Signal Processing: Modeling, Detection and Estimation, Ellicott City, MD, USA: Springer, 2019.

[19] M. Ainslie, Principles of sonar performance modeling, Heidelberg: Springer, 2010.

[20] K. Pelekanakis, A. Kondi, A. Russo and S. Carniel, "Simulation of Climate Change Impact on Underwater Acoustic Transmission Loss," in *IEEE/MTS OCEANS*, Singapore, 2024.

[21] V. Oppeneer, A. Schäfke, D. Brooker and M. Prior, “Detection Range of a Passing Emitter of Underwater sound,” *Journal of the Acoutical Society of America,* p. 1, 2024.

[22] J. Ridley, M. Menary, T. Kuhlbrodt, M. Andrews and T. Andrews, *MOHC HadGEM3-GC31-LL model output prepared for CMIP6 CMIP historical,* Earth System Grid Federation, 2019.

[23] R. J. Haarsma, M. J. Roberts, P. L. Vidale, C. A. Senior, A. Bellucci and a. et, “High Resolution Model Intercomparison Project (HighResMIP v1.0) for CMIP6,” *Geoscientific Model Development,* vol. 9, p. 4185–4208, November 2016.

[24] K. Riahi, S. Rao, V. Krey, C. Cho, V. Chirkov, G. Fischer, G. Kindermann, N. Nakicenovic and P. Rafaj, “RCP 8.5—A scenario of comparatively high greenhouse gas emissions,” *Climatic Change,* vol. 109, p. 33–57, August 2011.

[25] E. Galanaki, K. Lagouvardos, V. Kotroni, E. Flaounas and A. Argiriou, “Thunderstorm climatology in the Mediterranean using cloud-to-ground lightning observations,” *Atmospheric Research,* vol. 207, pp. 136-144, 2018.

[26] C. Harrison, “CANARY: A Simple Model of Ambient Noise and Coherence,” *Applied Acoustics,* vol. 51, no. 3, pp. 289-315, 1997.

[27] A. MacGillivray and C. de Jong, “A Reference Spectrum Model for Estimating Source Levels of Marine Shipping Based on Automated Identification System,” *Journal of Marine Science and Engineering,* vol. 9, no. 369, pp. 1-15, 2021.

[28] J. Brandon, K. Heaney, K. Seger, V. C., M. Schuster, A. Dumbrille and M. Lancaster, “PAME: Underwater noise pollution from shipping in the Arctic,” Arctic Council Secretariat, Tromso, Norway, 2021.

[29] M. Collins, “A split-step Padé solution for the parabolic equation method,” *Journal of the acoustical society of America,* vol. 93, pp. 1736-1742, 1993.

[30] I. Hartstra, M. Colin and M. Prior, “Active sonar performance modelling for Doppler-sensitive pulses,” *Journal of the Acoustical Society of America,* vol. 44, 2021.

[31] L. Possenti, G. Reichart, L. de Nooijer, F. Lam, C. de Jong, M. Colin, B. Binnerts and A. von der Heydt, “Predicting the contribution of climate change on North Atlantic underwater sound propagation,” *PeerJ,* vol. 11, no. e16208, 2023.

[32] G. A. Meehl, G. J. Boer, C. Covey, M. Latif and R. J. Stouffer, “The Coupled Model Intercomparison Project (CMIP),” *Bulletin of the American Meteorological Society,* vol. 81, p. 313–318, February 2000.

[33] Q. Ding, A. Schweiger, M. L’Heureux, D. Battisti, S. Po-Chedley, N. Johnson, E. Blanchard-Wrigglesworth, K. Harnos, Q. Zhang, R. Eastman and E. Steig, “Influence of high-latitude atmospheric circulation changes on summertime Arctic sea ice,” *Nature Climate Change,* vol. 7, p. 289–295, March 2017.

[34] G. Danabasoglu, S. C. Bates, B. P. Briegleb, S. R. Jayne, M. Jochum, W. G. Large, S. Peacock and S. G. Yeager, “The CCSM4 Ocean Component,” *Journal of Climate,* vol. 25, p. 1361–1389, March 2012.

[35] M. Årthun, T. Eldevik, L. H. Smedsrud, Ø. Skagseth and R. B. Ingvaldsen, “Quantifying the Influence of Atlantic Heat on Barents Sea Ice Variability and Retreat*,” *Journal of Climate,* vol. 25, p. 4736–4743, July 2012.

[36] K. C. Armour, I. Eisenman, E. Blanchard-Wrigglesworth, K. E. McCusker and C. M. Bitz, “The reversibility of sea ice loss in a state-of-the-art climate model: SEA ICE REVERSIBILITY,” *Geophysical Research Letters,* vol. 38, p. n/a–n/a, August 2011.

[37] A. Nummelin, M. Ilicak, C. Li and L. H. Smedsrud, “Consequences of future increased Arctic runoff on Arctic Ocean stratification, circulation, and sea ice cover,” *Journal of Geophysical Research: Oceans,* vol. 121, p. 617–637, January 2016.

[38] E. P. Metzner, M. Salzmann and R. Gerdes, “Arctic Ocean Surface Energy Flux and the Cold Halocline in Future Climate Projections,” *Journal of Geophysical Research: Oceans,* vol. 125, February 2020.

[39] G. Wenz, “Acoustic ambient noise in the ocean: Spectra and sources,” *Journa of the Acoustic Society of America,* vol. 34, pp. 1936-1956, 1962.